Journal of Computer Assisted Tomography
15(6):915–922, November/December

Localized Proton NMR Spectroscopy of Brain Tumors Using Short-Echo Time STEAM Sequences

Jens Frahm, Harald Bruhn, Wolfgang Hänicke, Klaus-Dietmar Merboldt, Kay Mursch, and Evangelos Markakis

Abstract: Recent progress in localized proton NMR spectroscopy has been utilized to improve the spatial resolution and the metabolic specificity in a study of 19 patients with intracranial tumors. Selected examples demonstrate that short echo time stimulated echo acquisition mode sequences are able (a) to account for macroscopic tissue heterogeneity by reducing the volume of interest to 2–8 ml and (b) to facilitate a reasonable characterization of tumor metabolism by increasing the number of accessible metabolites. Proton NMR spectra were acquired within measuring times of 6.5 min on a 2.0 T whole-body system using the imaging headcoil. **Index Terms:** Magnetic resonance imaging, spectroscopy—Brain, neoplasms—Magnetic resonance imaging, tissue characterization.

Localized proton NMR spectroscopy (MRS) has revealed a considerable potential for unique noninvasive insights into brain metabolism under both normal and pathologic conditions. Although the clinical applicability ranges from focal diseases, e.g., multiple sclerosis or infarcts, to global neurodegenerative processes of gray or white matter, initial studies focused on metabolic investigations of intracranial tumors (1–12). Although these first efforts have already demonstrated striking alterations of the metabolite pattern in tumors as compared with normal brain tissue, most MRS studies are hampered by two major methodologic problems.

First, the commonly used localization sequences require the use of long echo times (TE) of 135–270 ms (a) to obtain sufficiently large water suppression factors and (b) to avoid instrumental shortcomings such as residual eddy currents following the application of magnetic field gradients for localization. As a consequence of the long delay between excitation and detection, T2 relaxation of the metabolite resonances causes a significant loss in signal-to-noise ratio (SNR). To compensate for this drawback while retaining reasonable investigational times, early investigators increased the volume of interest (VOI) to 27–200 ml. In most cases, this compromised the spectroscopic results by considerable partial volume effects with normal brain tissue.

Second, the T2 relaxation process leads to a total loss of metabolites with relaxation times $3 \times T2 \leq TE$, e.g., mobile lipids. It further complicates and often precludes a reliable identification of those resonances that are strongly spin-coupled at field strengths of 1.0–2.0 T. This is due to the fact that the complex signal modulation associated with increasing TE leads to an irreversible dephasing of the distorted multiplet resonances. Typical examples originate from the methylene groups of glutamate and glutamine. The methyl doublet resonances of lactate and alanine represent the only exceptions of weak coupling.

The use of state-of-the-art hardware and recent progress in the development of stimulated echo acquisition mode (STEAM) spectroscopy sequences have resulted in technical improvements with respect to water suppression, short TE, and small volumes (13). The purpose of the present study is to

From the Max-Planck-Institut für biophysikalische Chemie (J. Frahm, H. Bruhn, W. Hänicke, and K.-D. Merboldt) and the Neurochirurgische Klinik, Universität Göttingen (K. Mursch and E. Markakis), Göttingen, Germany. Address correspondence and reprint requests to Dr. J. Frahm at Max-Planck-Institut für biophysikalische Chemie, Postfach 2841, D-3400 Göttingen, Germany.

explore the clinical utility of pertinent advances in dealing with practical problems such as tissue heterogeneity and metabolic specificity. The results are expected to guide future studies aimed at new insights into the pathophysiology of tumor metabolism in the intact living organism.

MATERIALS AND METHODS

Magnetic Resonance Imaging

All studies were performed at 2.0 T (Siemens Magnetom, Erlangen, Germany) using the imaging headcoil and standard gradient system (10 mTm^{-1} maximum strength) for both MRI and MRS. Clinical imaging and selection of the VOI was accomplished with use of a fast scan MR protocol (14) combining T1-weighted fast low angle shot images [repetition time (TR)/TE 100/6 ms, 70° flip angle, one excitation] and T2-weighted CE-FAST images (TR/TE 22/−9 ms, 45–60° flip angle, 2 excitations). During the course of the study the parameters for the CE-FAST sequence were slightly modified to reduce the motion sensitivity of the images (TR/TE 13.8/−6 ms, 40° flip angle, 4 excitations). All images were acquired with a 4 mm slice thickness and a 256 × 256 matrix covering a 250 mm field of view. The total investigational time for imaging was <10 min.

Magnetic Resonance Spectroscopy

Localized proton NMR spectra were acquired using STEAM sequences with TE of 20–270 ms, VOI sizes of 2–8 ml, and within measuring times of 6.5 min (TR = 3,000, 128 scans). Technical details have been reported elsewhere (13). Reconstruction of spectra included zero filling (2K complex data points to 4K) and gaussian filtering (1.2 Hz line broadening) of the raw data followed by one-dimensional Fourier transformation and zero- and first-order phase correction. No baseline correction, smoothing algorithm, or resolution enhancement was applied.

Patients and Controls

Patients were primarily selected for evaluating the relevance of applicational aspects of image-guided proton MRS. A number of neoplasms of different location, size, shape, and histology were investigated to assess the influence of the VOI size and tissue composition for the development of reliable metabolic "fingerprints." Nineteen patients were studied, including 12 with astrocytomas (grades II–IV), two with meningiomas, two acoustic neurinomas, one pituitary adenoma, one ependymoma, and one metastasis of a bronchial carcinoma. In most cases histopathologic classification was available after surgery. Written informed consent was obtained in all cases prior to the NMR investigation.

Control spectra of healthy subjects were available from ~300 proton MRS brain studies. Figure 1 shows representative spectra of normal white matter (12 ml VOI, TR 3,000 ms, 128 scans) from the parietal cortex of a 23-year-old female control at two TEs. The spectrum with the long TE at 270 ms (Fig. 1a) is dominated by the singlet methyl resonances of *N*-acetylaspartate (NAA: 2.01 ppm), phosphocreatine and creatine (Cr: 3.03, 3.94 ppm), and choline-containing compounds (Cho: 3.22 ppm). As a benefit of reduced T2 signal losses and effective elimination of spin-coupling modulation,

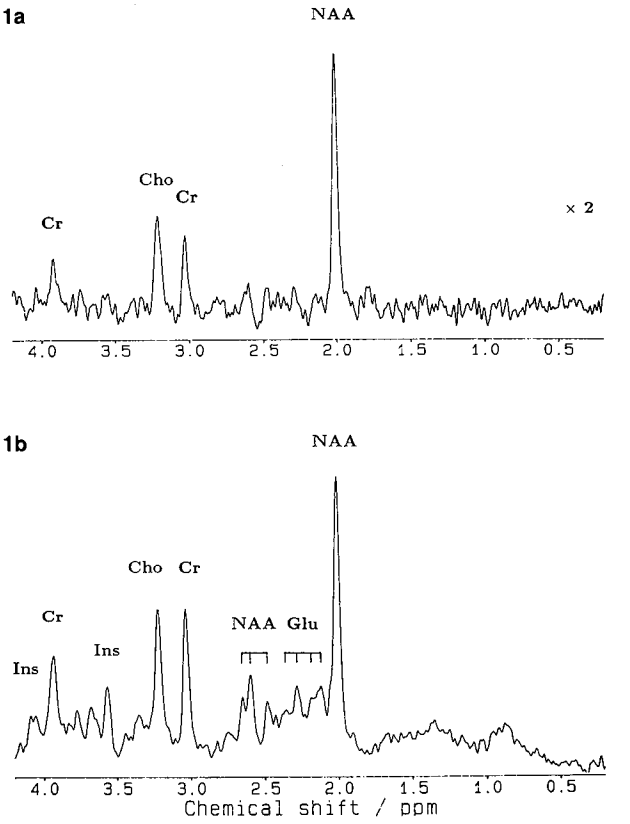

FIG. 1. Proton NMR spectra (2.0 T) of white matter localized in the right parietal cortex of a 23-year-old woman control at TE **(a)** 270 ms and **(b)** 20 ms. Both spectra were acquired with 12 ml VOI (20 × 30 × 20 mm^3) within measuring times of 6.5 min each (TR 3,000 ms, 128 scans). Spectrum (a) has been multiplied by a factor of two relative to (b). Resonances refer to *N*-acetylaspartate (NAA), glutamate (Glu), creatine and phosphocreatine (Cr), choline-containing compounds (Cho), and *myo*-inositol (Ins).

the short TE spectrum at 20 ms (Fig. 1b) exhibits further resonances from glutamate (Glu: 2.11, 2.18, 2.28, 2.36 ppm; 3.70, 3.77, 3.84 ppm), the aspartyl-group of NAA (2.48, 2.60, 2.64 ppm), and *myo*-inositol (Ins: 3.56, 4.08 ppm) with a frequency reproducibility of ±0.01 ppm (15).

Although quantification of absolute concentrations has been achieved in a homogeneous group of young adults (16), it is more difficult in an arbitrary group of patients due to different head sizes and corresponding changes in the radiofrequency coil loading factors. The total area of the NAA methyl resonance in white matter (Fig. 1b) refers to an in vivo concentration of ~10 m*M* including 1–2 m*M* from a corresponding resonance of the dipeptide *N*-acetylaspartylglutamate (16,17). The physiologic concentrations of cerebral lactate (Lac: 1.33 ppm) and glucose (3.43, 3.80 ppm) of ~1 m*M* are rarely detected in healthy tissue under the chosen experimental conditions. Moreover, the spectra lack resonances from fatty acids (e.g., triglycerides) but show minor humps in the 0.8–0.9 and 1.2–1.3 ppm ranges that may be due to mobile lipids (e.g., cholesterol), residues of cytosolic proteins, and/or branched amino acids.

RESULTS

Figure 2 shows spectra at different TEs and with different VOI sizes from a 64-year-old woman who had an astrocytoma grade III. In agreement with

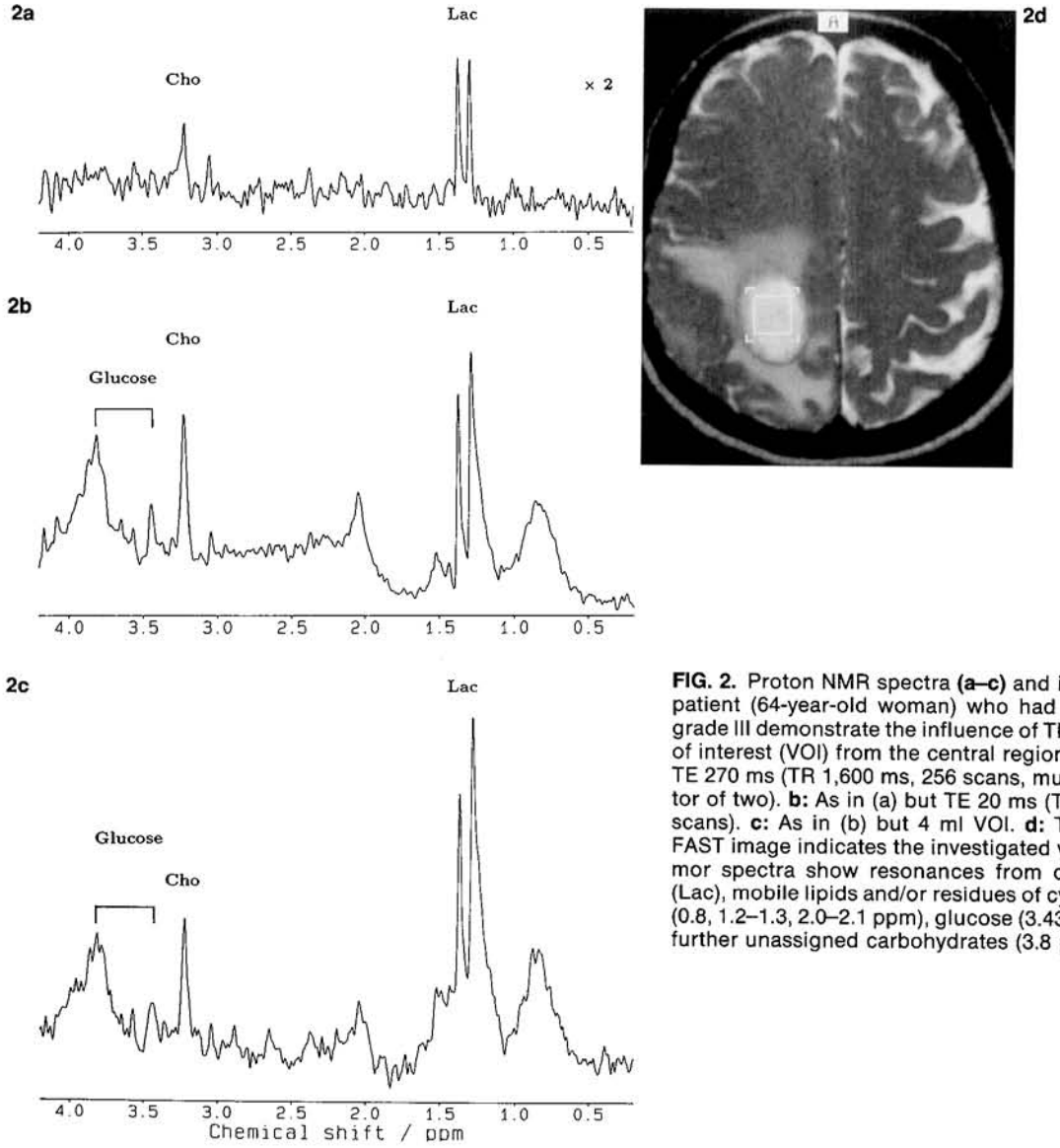

FIG. 2. Proton NMR spectra **(a–c)** and image **(d)** from a patient (64-year-old woman) who had an astrocytoma grade III demonstrate the influence of TE. **a:** 8 ml volume of interest (VOI) from the central region of the tumor at TE 270 ms (TR 1,600 ms, 256 scans, multiplied by a factor of two). **b:** As in (a) but TE 20 ms (TR 1,500 ms, 256 scans). **c:** As in (b) but 4 ml VOI. **d:** T2-weighted CE-FAST image indicates the investigated volumes. The tumor spectra show resonances from cholines, lactate (Lac), mobile lipids and/or residues of cytosolic proteins (0.8, 1.2–1.3, 2.0–2.1 ppm), glucose (3.43, 3.80 ppm), and further unassigned carbohydrates (3.8 ppm).

previous findings the spectrum at the long TE 270 ms (8 ml VOI, Fig. 2a) displays a metabolite pattern believed to be characteristic of high grade astrocytomas: strongly elevated lactate, some contributions from cholines, a complete absence of NAA found in normal neuronal tissue (compare Fig. 1), and very little if any creatines. A reduction of TE to 20 ms (same VOI, Fig. 2b) yields a considerable improvement in SNR and allows the detection of additional metabolites. In fact, further resonances are due to mobile lipids (0.8, 1.2–1.3, 2.0–2.1 ppm) and yet unassigned carbohydrates (3.8 ppm), both with short T2 relaxation times. Elevated glucose levels in the tumorous tissue become observable by two strongly coupled resonances at 3.43 and 3.80 ppm. In this case a rather homogeneous regional distribution of metabolites is indicated by a further reduction of the VOI to 4 ml at the same location. The corresponding spectrum (Fig. 2c) is largely comparable with that in the 8 ml VOI (Fig. 2b) but exhibits even more lactate and less choline. This finding reflects the increased contribution of necrosis in the center of the astrocytoma (Fig. 2d).

The influence of a partial volume effect between normal and tumorous tissue is demonstrated in Fig. 3 for the case of a 33-year-old man who had an astrocytoma grade II (partly grade III in cyst). Even though a relatively small VOI of 8 ml may not be expected to result in significant contributions from normal brain tissue according to the appearance of the lesion on MR (Fig. 3c), the corresponding spectrum contains a residual signal from NAA (Fig. 3a). This signal only disappeared after reduction of the VOI size to 2 ml, i.e., a 12.6 × 12.6 × 12.6 mm^3 cube (Fig. 3b). Thus, the occurrence of NAA in the 8 ml spectrum must not be misunderstood as being representative of the metabolic state of the tumor proper rather than of residual vital neurons present in the adjacent edematous zone infiltrated by tumor cells. No lactate and lipids were observed either in the solid mass or in the cystic part (not shown).

In a further example, Fig. 4 demonstrates the influence of TE in a 52-year-old patient who had a glioblastoma (astrocytoma grade IV). Although the long TE results in a spectrum containing cholines exclusively (Fig. 4a), a reduction of TE to 20 ms yields additional contributions from mobile lipids and prominent resonances from *myo*-inositol. Since cholines and inositol are precursors of membrane lipids, their elevated concentrations may be indica-

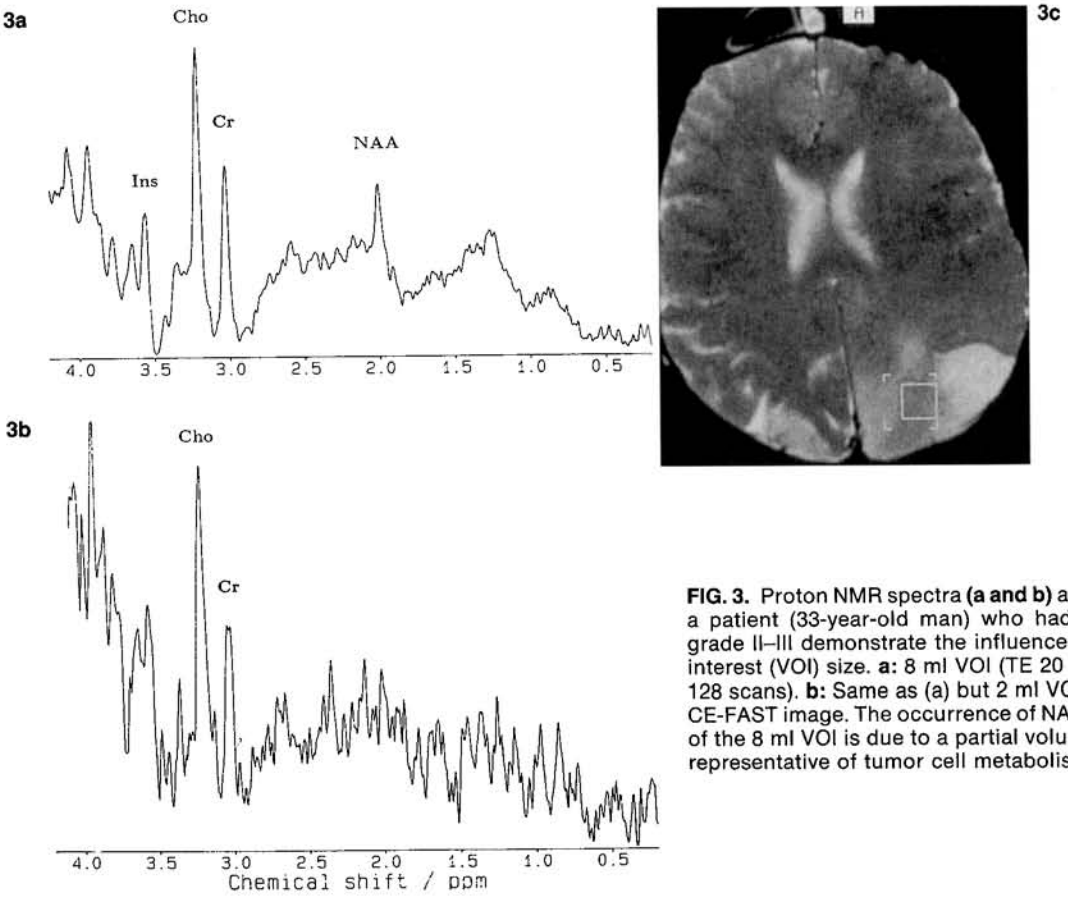

FIG. 3. Proton NMR spectra **(a and b)** and image **(c)** from a patient (33-year-old man) who had an astrocytoma grade II–III demonstrate the influence of the volume of interest (VOI) size. **a:** 8 ml VOI (TE 20 ms, TR 3,000 ms, 128 scans). **b:** Same as (a) but 2 ml VOI. **c:** T2-weighted CE-FAST image. The occurrence of NAA in the spectrum of the 8 ml VOI is due to a partial volume effect and not representative of tumor cell metabolism.

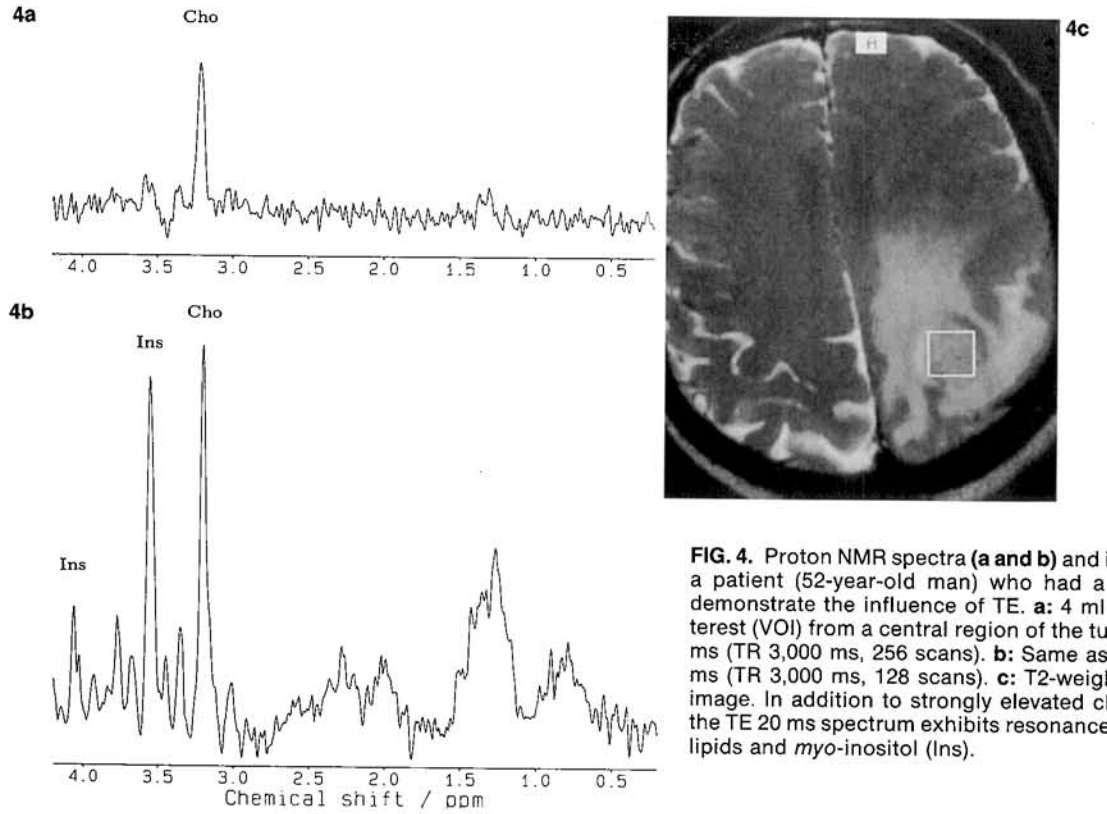

FIG. 4. Proton NMR spectra **(a and b)** and image **(c)** from a patient (52-year-old man) who had a glioblastoma demonstrate the influence of TE. **a:** 4 ml volume of interest (VOI) from a central region of the tumor at TE 270 ms (TR 3,000 ms, 256 scans). **b:** Same as (a) but TE 20 ms (TR 3,000 ms, 128 scans). **c:** T2-weighted CE-FAST image. In addition to strongly elevated cholines (Cho), the TE 20 ms spectrum exhibits resonances from mobile lipids and *myo*-inositol (Ins).

tive of enhanced membrane turnover associated with cell proliferation. The absence of lactate suggests a slow growth and/or adequate vascularization of the tumor precluding extensive anerobic glycolysis.

Figure 5 shows spectra of a 43-year-old man who had a parasagittal frontoparietal ependymoma surrounded by a large cystic region. The tumor had recurred 3 months after the first resection. As indicated in the T2-weighted image (Fig. 5d) MRS was performed in two locations: the hypointense tumor mass and the hyperintense cystic region, respectively. The resulting proton NMR spectrum of the solid tumor at TE 270 ms (Fig. 5a) exhibits a strong resonance from cholines and very little lactate. As in preceding examples the corresponding TE 20 ms spectrum (Fig. 5b) not only benefits from a significant gain in SNR but, more importantly, unravels additional metabolite resonances from *myo*-inositol and mobile lipids as major constituents of the vital part of the recurrent tumor. When shifting the VOI to the cystic region, the spectrum (Fig. 5c) lacks most of the contributions from cholines and inositol but adds lactate on top of the resonances from mobile lipids as well as some glucose. The altered metabolite composition of the cyst reflects less pronounced or no cell proliferation as well as anerobic glycolysis in the residual and probably necrotic tissue.

Finally, in the case of a 62-year-old man who had a metastasis of bronchial carcinoma shown in Figure 6, the series of TE 20 ms spectra from three locations reveals remarkable metabolic heterogeneity. The central metastasis is predominantly characterized by elevated lactate and mobile lipids (Fig. 6c), and the two spectra from a frontal (Fig. 6a) and dorsal location (Fig. 6b) result in distinct metabolite patterns. Although both areas appear as similar edematous regions on MR (Fig. 6d), the frontal tissue exhibits a 40–50% loss of NAA and no increase of lactate, whereas the dorsal VOI shows considerably enhanced neuronal damage and impaired energy metabolism verified by a further reduction of NAA and a significant increase of lactate. Obviously, this regional variability provides additional information on the preferred area of the tumor invasion. In both cases adjacent brain parenchyma exhibit an overall reduction in signal partly due to the diluting effect of the edema. The complete loss of *myo*-inositol is not yet understood.

DISCUSSION

The prototype for focal diseases of the brain are tumors. The selection of a well-matched VOI for spectroscopy in a space-occupying lesion should

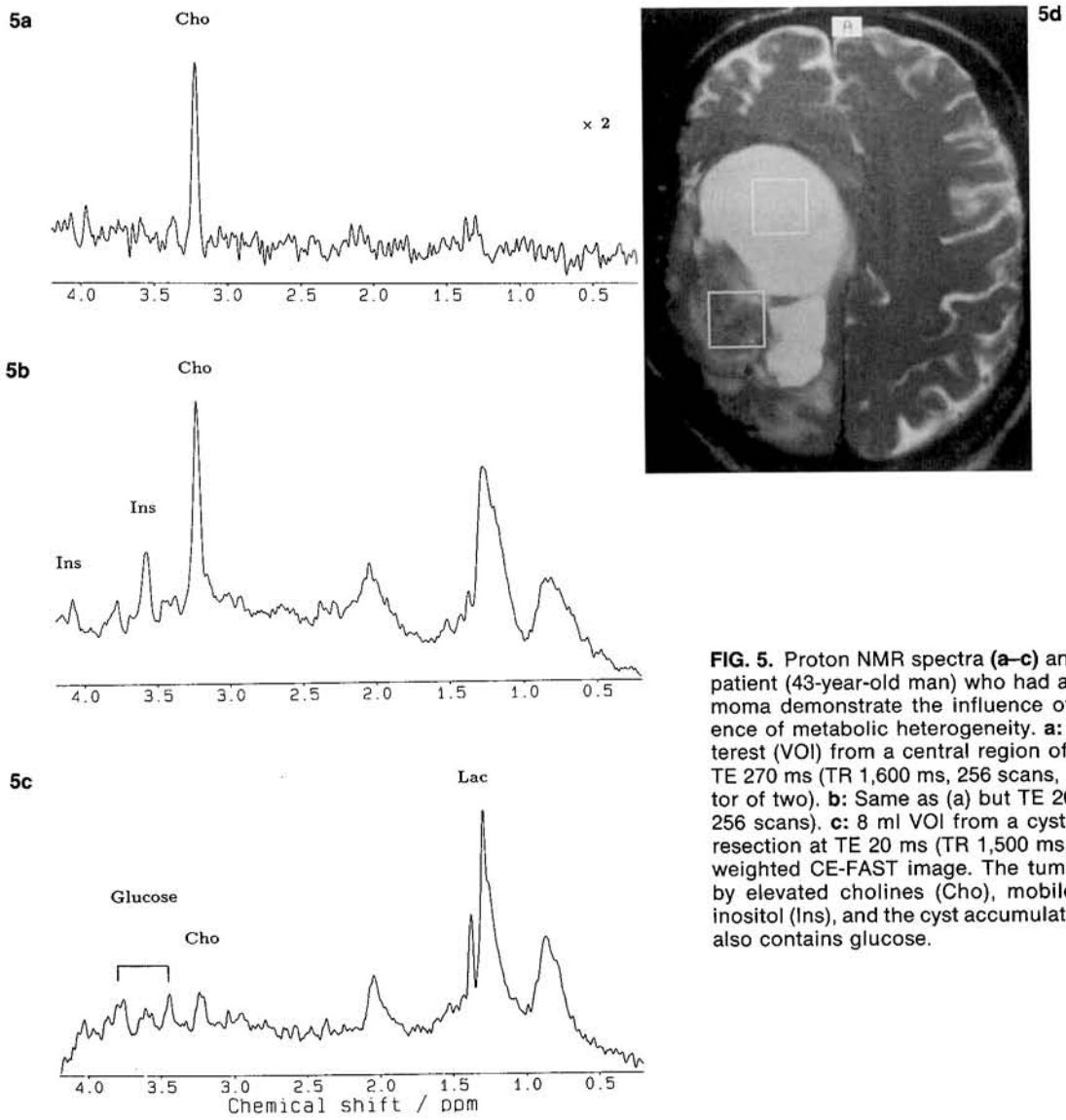

FIG. 5. Proton NMR spectra **(a–c)** and image **(d)** from a patient (43-year-old man) who had a recurring ependymoma demonstrate the influence of TE and the presence of metabolic heterogeneity. **a:** 8 ml volume of interest (VOI) from a central region of the solid tumor at TE 270 ms (TR 1,600 ms, 256 scans, multiplied by a factor of two). **b:** Same as (a) but TE 20 ms (TR 1,500 ms, 256 scans). **c:** 8 ml VOI from a cystic region after first resection at TE 20 ms (TR 1,500 ms, 256 scans). **d:** T2-weighted CE-FAST image. The tumor is characterized by elevated cholines (Cho), mobile lipids, and *myo*-inositol (Ins), and the cyst accumulates lactate (Lac) and also contains glucose.

pose no problem. However, selected clinical cases demonstrate that the use of a sufficiently small VOI for localized MRS is essential to eliminate partial volume effects with normal brain tissue (Fig. 3) and to account for metabolic tissue heterogeneity inside or around a lesion (Figs. 5 and 6). Obviously, the assessment of the metabolism of the active tumor rather than a characterization compromised by necrotic tissue or edematous parenchyma must be a prerequisite for further medical conclusions, e.g., the extent of surgery or other therapeutic interventions.

A second important result is the improved tissue specificity that may evolve from the increased number of accessible metabolites. A typical example is given by Figs. 4a and 5a showing identical spectra from a glioblastoma and a recurrent ependymoma at TE 270 ms. In contrast, the corresponding spectra at TE 20 ms (Figs. 4b and 5b) unravel a marked difference demonstrating a prominent concentration of *myo*-inositol in the glioblastoma. One may presume that differentiation of high grade astrocytomas from other pathologies involving neuronal degeneration and lactate production will be facilitated as well.

In conclusion, the methodologic advances of short TE proton MRS translate into improved spatial resolution and enhanced metabolic specificity for the noninvasive characterization of primary and secondary brain tumors.

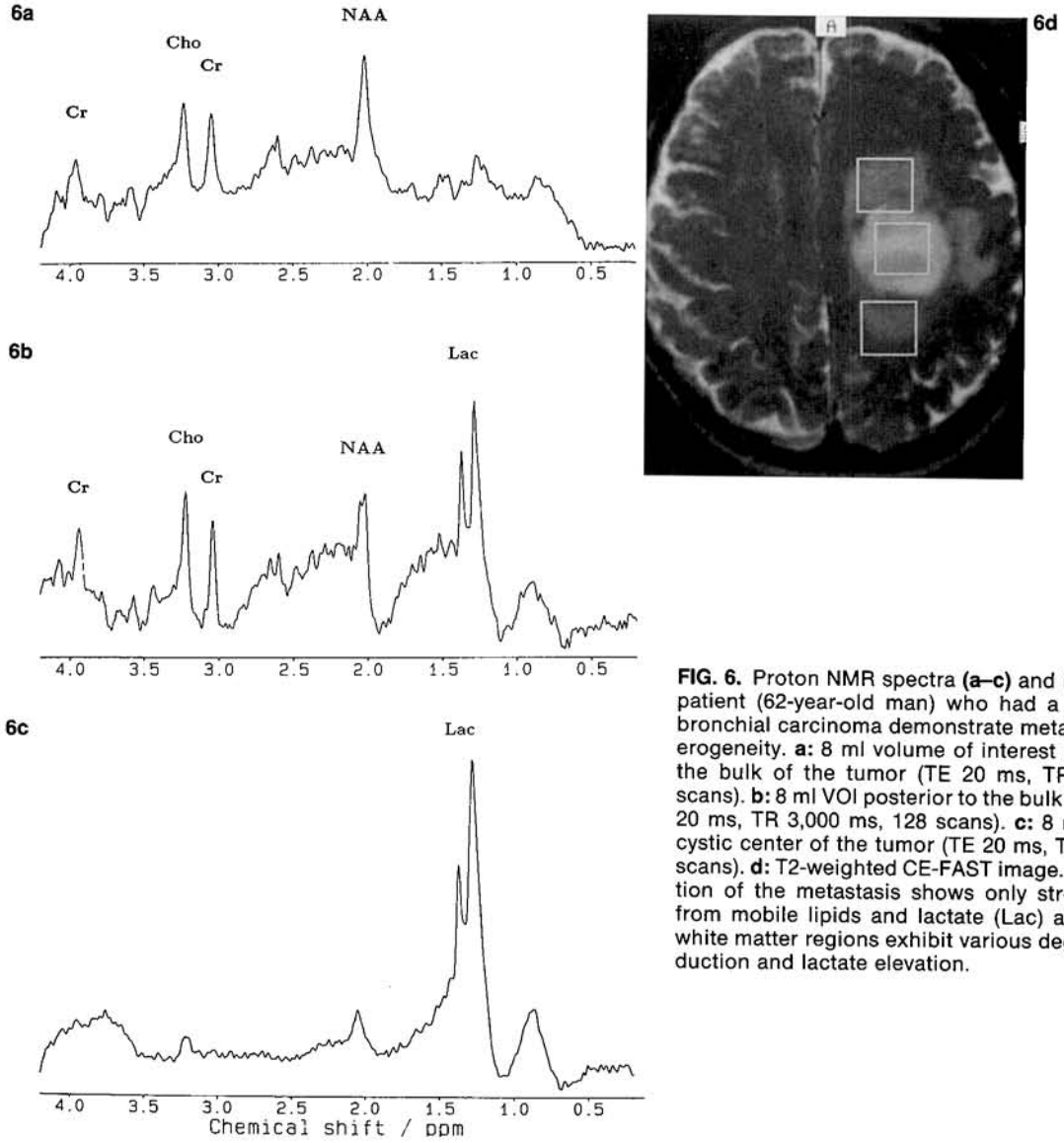

FIG. 6. Proton NMR spectra **(a–c)** and image **(d)** from a patient (62-year-old man) who had a metastasis of a bronchial carcinoma demonstrate metabolic tissue heterogeneity. **a:** 8 ml volume of interest (VOI) anterior to the bulk of the tumor (TE 20 ms, TR 3,000 ms, 128 scans). **b:** 8 ml VOI posterior to the bulk of the tumor (TE 20 ms, TR 3,000 ms, 128 scans). **c:** 8 ml VOI from the cystic center of the tumor (TE 20 ms, TR 1,500 ms, 256 scans). **d:** T2-weighted CE-FAST image. The central portion of the metastasis shows only strong resonances from mobile lipids and lactate (Lac) and the adjacent white matter regions exhibit various degrees of NAA reduction and lactate elevation.

Acknowledgment: Financial support by the Bundesminister für Forschung und Technologie (BMFT) of the Federal Republic of Germany (Grant 01 VF 8606/6) is gratefully acknowledged.

REFERENCES

1. Bruhn H, Frahm J, Gyngell ML, et al. Noninvasive differentiation of tumors with use of localized H-1 MR spectroscopy in vivo. Initial experience in patients with cerebral-tumors. *Radiology* 1989;172:541–8.
2. Langkowski JH, Wieland J, Bomsdorf H, et al. Preoperative localized in vivo proton spectroscopy in cerebral tumors at 4.0 Tesla—first results. *Magn Reson Imaging* 1989;7:547–55.
3. Alger JR, Frank JA, Bizzi A, et al. Metabolism of human gliomas: assessment with H-1-MR spectroscopy and F-18 fluorodeoxyglucose PET. *Radiology* 1990;177:633–41.
4. Arnold DL, Shoubridge EA, Villemure JG, Feindel W. Proton and phosphorus magnetic resonance spectroscopy of human astrocytomas in vivo. Preliminary observations on tumor grading. *NMR Biomed* 1990;3:184–9.
5. Bruhn H, Frahm J, Gyngell ML, et al. Noninvasive differentiation of tumors with use of localized H-1 spectroscopy in vivo: initial experience in patients with cerebral-tumors. Author's response. *Invest Radiol* 1990;25:1049–50.
6. Gill SS, Thomas DGT, Van Bruggen N, et al. Proton MR spectroscopy of intracranial tumours: in vivo and in vitro studies. *J Comput Assist Tomogr* 1990;14:497–504.
7. Henriksen O, Larsson H, Jensen KM. In vivo H-1 spectroscopy of the human brain at 1.5 Tesla. Preliminary experience at a clinical installation. *Acta Radiol [Diagn] (Stockh)* 1990; 31:181–6.
8. Luyten PR, Mariën AJH, Heindel W, et al. Metabolic imaging of patients with intracranial tumors: H-1 MR spectroscopic imaging and PET. *Radiology* 1990;176:791–9.
9. Sauter R, Loeffler W, Bruhn H, Frahm J. The human brain—localized H-1 MR spectroscopy at 1.0-T. *Radiology* 1990;176:221–4.

10. Segebarth CM, Balériaux DF, Luyten PR, den Hollander JA. Detection of metabolic heterogeneity of human intracranial tumors in vivo by 1H NMR spectroscopic imaging. *Magn Reson Med* 1990;13:62–76.
11. Sostman HD, Charles HC. Noninvasive differentiation of tumors with use of localized H-1 spectroscopy in vivo—initial experience in patients with cerebral-tumors. Critical review. *Invest Radiol* 1990;25:1047–8.
12. Demaerel P, Johannik K, Van Hecke P, et al. Localized ^{1}H NMR spectroscopy in fifty cases of newly diagnosed intracranial tumors. *J Comput Assist Tomogr* 1991;15:67–76.
13. Frahm J, Michaelis T, Merboldt KD, Bruhn H, Gyngell ML, Hänicke W. Improvements in localized proton NMR spectroscopy of human brain. Water suppression, short echo times, and 1 ml resolution. *J Magn Reson* 1990;90:464–73.
14. Frahm J, Gyngell ML, Hänicke W. Rapid scan techniques. In: Stark DD, Bradley WG, eds. *Magnetic resonance imaging*. 2nd ed. St Louis: CV Mosby, 1991.
15. Michaelis T, Merboldt KD, Hänicke W, Gyngell ML, Bruhn H, Frahm J. On the identification of cerebral metabolites in localized proton NMR spectra of the normal human brain in vivo. *NMR Biomed* 1991;4:90–8.
16. Michaelis T, Bruhn H, Gyngell ML, Hänicke W, Merboldt KD, Frahm J. Quantification of cerebral metabolites in man. Results using short-echo time localized proton MRS. In: *Abstracts, Society of Magnetic Resonance in Medicine* 10th annual meeting and exhibition, August 10–16, 1991. San Francisco, CA: Society of Magnetic Resonance in Medicine, 387.
17. Frahm J, Michaelis T, Merboldt KD, Hänicke W, Gyngell ML, Bruhn H. On the *N*-acetyl methyl resonance in localized ^{1}H-NMR spectra of human brain in vivo. *NMR Biomed* (in press).